



Research papers

A combined triggering-propagation modeling approach for the assessment of rainfall induced debris flow susceptibility



Laura Maria Stancanelli ^{*}, David Johnny Peres, Antonino Cancelliere, Enrico Foti

Department of Civil Engineering and Architecture, University of Catania, Catania, Italy

ARTICLE INFO

Article history:

Received 2 March 2017

Received in revised form 11 April 2017

Accepted 15 April 2017

Available online 28 April 2017

This manuscript was handled by K.

Georgakakos, Editor-in-Chief

Keywords:

Susceptibility assessment

Debris flow

Triggering modeling

Propagation modeling

TRIGRS

Giampileri

ABSTRACT

Rainfall-induced shallow slides can evolve into debris flows that move rapidly downstream with devastating consequences. Mapping the susceptibility to debris flow is an important aid for risk mitigation. We propose a novel practical approach to derive debris flow inundation maps useful for susceptibility assessment, that is based on the integrated use of DEM-based spatially-distributed hydrological and slope stability models with debris flow propagation models. More specifically, the TRIGRS infiltration and infinite slope stability model and the FLO-2D model for the simulation of the related debris flow propagation and deposition are combined. An empirical instability-to-debris flow triggering threshold calibrated on the basis of observed events, is applied to link the two models and to accomplish the task of determining the amount of unstable mass that develops as a debris flow. Calibration of the proposed methodology is carried out based on real data of the debris flow event occurred on 1 October 2009, in the Peloritani mountains area (Italy). Model performance, assessed by receiver-operating-characteristics (ROC) indexes, evidences fairly good reproduction of the observed event. Comparison with the performance of the traditional debris flow modeling procedure, in which sediment and water hydrographs are inputted as lumped at selected points on top of the streams, is also performed, in order to assess quantitatively the limitations of such commonly applied approach. Results show that the proposed method, besides of being more process-consistent than the traditional hydrograph-based approach, can potentially provide a more accurate simulation of debris-flow phenomena, in terms of spatial patterns of erosion and deposition as well on the quantification of mobilized volumes and depths, avoiding overestimation of debris flow triggering volume and, thus, of maximum inundation flow depths.

© 2017 Elsevier B.V. All rights reserved.

1. Introduction

Rainfall induced landslides and debris flows are among the most damaging natural hazards (Bogaard and Greco, 2016; Sidle and Ochiai, 2006). Each year landslides cause thousands of casualties and billions of dollars in damages across the world (Highland and Bobrowsky, 2008; Farahmand and AghaKouchak, 2013). Furthermore, under certain conditions shallow landslides may evolve into debris flows, causing devastating effects on downstream areas.

Effective landslide risk mitigation strategies start from the estimation of debris flow susceptibility, i.e. likelihood of debris flow occurrence and the extension of the area potentially affected by propagation and deposition of the mobilized mass. Indeed, susceptibility estimation is an essential step for the assessment of landslide risk and for the identification of appropriate structural

and/or non structural mitigation measures. To this end, debris flow triggering and propagation models represent useful tools (Jakob, 2005; Hürlimann et al., 2008), since they enable to build up reliable inundations maps.

Traditional assessment of debris flows propagation requires the definition of an initiation scenario as well as the characterization of the rheology of the moving mass (Mergili et al., 2012). The former task is generally carried out through the estimation of an hydrograph, incremented by a suitable coefficient to account for the solid fraction transported by the debris flow (e.g., Rickenmann et al., 2006; Stancanelli et al., 2015; Lanzoni et al., 2017), or, alternatively, through the definition of an event magnitude based on sediment instability. Characterization of the rheology entails the choice of suitable rheological laws, to describe the specific sediment–water mixture subject to movement.

The definition of the event scenario through a hydrograph-based procedure, however, presents two main weak points. First of all, the input is not spatially distributed, since the hydrograph is usually given at some user-defined points. Furthermore, the

^{*} Corresponding author.

E-mail address: lmstanca@dica.unict.it (L.M. Stancanelli).

estimate of the magnitude of the event is often quite uncertain, as it is based on empirical relationship. Thus, the resulting propagation may be affected by significant errors.

On the other hand, various physically based hydrological and slope stability models have been developed to model landslide triggering, also in a spatially distributed fashion (Montgomery and Dietrich, 1994; Baum et al., 2002; Baum et al., 2008; Baum et al., 2010; D'Odorico et al., 2005; Iverson, 2000; Rosso et al., 2006; Milledge et al., 2014). Such models essentially compute on a DEM basis cells which are likely unstable (and thus can potentially trigger a debris flow) in response to rainfall events, given initial soil moisture conditions. Such models also find application to determine landslide triggering thresholds for early warning (Rosso et al., 2006; Salciarini et al., 2008; Peres and Cancelliere, 2014).

In this paper, a debris flow susceptibility assessment approach which combines spatially-distributed hydrological model and slope stability analysis with debris flow propagation and deposition models is proposed.

More specifically, the TRIGRS saturated model (Baum et al., 2002; Baum et al., 2008), is combined with FLO-2D model for simulating debris flow propagation and deposition (O'Brien, 2006). TRIGRS, based on simplifications of the Richards' equation (Iverson, 2000) enables to compute the watershed cells subject to geomechanical instability in response to rainfall and has been successfully applied to assess landslide initiation in different case-study areas (Peres and Cancelliere, 2016; Peres and Cancelliere, 2014; Salciarini et al., 2008; Baum et al., 2002; Baum et al., 2008; Baum et al., 2010; Schilirò et al., 2015).

Although in principle, use of the outcome of hydrological and slope stability models, namely the potentially unstable cells, as input to propagation models could appear as a straightforward exercise, however this is seldom the case since generally not all of the potentially unstable cells (identified by the triggering models) evolve into landslide and debris flows. In order to overcome such a problem, a topography-based instability-to-debris flow triggering threshold is applied to the output of the TRIGRS model, and the identified triggered cells are here used as a spatially-distributed input to the FLO-2D model for simulating debris flow propagation and deposition.

The resulting framework is quite general and is independent from the specific triggering and propagation models adopted. Furthermore, the procedure is in principle more process-consistent than the use of hyper-concentrated hydrographs as input to the FLO-2D model, and may find application also to predict future debris flow initiation and propagation.

The methodology is applied to the well documented debris flow event occurred at Giampilieri (Italy) on 1 October 2009. The results of such application are then compared to those provided by the traditional approach, where the input to the propagation model is as an hyper-concentrated flow hydrograph whose total volumes are those resulting from the application of the TRIGRS and instability-to-debris flow triggering threshold, in order to evaluate uncertainty related to the use of single input points rather than a spatially distributed input.

A comparison of the derived debris flow volumes with those computed by well-known empirical relationships is also carried out, for a more complete assessment of the performance of the proposed rainfall infiltration and geotechnical instability model application.

Paper outline is as follows. In Section 2 the methodology for integrated debris flow susceptibility assessment is illustrated as well as the proposed approach to identify the unstable cells among the potentially unstable ones. Section 3 describes the case-study area and the alluvial event of October 1st, 2009, the available data and the debris flow susceptibility assessment, and discusses the

results in terms of inundation map, comparing present integrated spatially-distributed-input approach and the traditional method, and analysing their performance. Finally, Section 4 presents the conclusions and outlooks for further developments.

2. Material and methods

2.1. Rainfall infiltration and geotechnical instability model

To identify the unstable cells of a given catchment, in response to a given rainfall event, we use a model based on the TRIGRS v.1 software (Baum et al., 2002; Baum et al., 2008; Baum et al., 2010). The resulting unstable domain is then filtered to estimate the cells that will likely contribute to debris flow formation (Section 2.3).

A sketch of a typical digital terrain model cell used in the computations is shown in Fig. 1.

The pressure head ψ at a given depth Z and time instant t of each cell in response to a given rainfall event $I_{n,Z}$ $n = 1, 2, \dots, N$, for given initial conditions (i.e., an initial water table depth d), reads:

$$\begin{aligned} \psi(Z, t) = & (Z - d)\beta + \\ & 2 \sum_{n=1}^N \frac{I_{n,Z}}{K_S} H(t - t_n) [D_1(t - t_n)]^{1/2} \cdot \\ & \sum_{m=1}^{\infty} \left\{ \operatorname{ierfc} \left[\frac{(2m-1)d_{LZ} - (d_{LZ} - Z)}{2[D_1(t - t_n)]^{1/2}} \right] + \operatorname{ierfc} \left[\frac{(2m-1)d_{LZ} + (d_{LZ} - Z)}{2[D_1(t - t_n)]^{1/2}} \right] \right\} - \\ & 2 \sum_{n=1}^N \frac{I_{n,Z}}{K_S} H(t - t_{n+1}) [D_1(t - t_{n+1})]^{1/2} \cdot \\ & \sum_{m=1}^{\infty} \left\{ \operatorname{ierfc} \left[\frac{(2m-1)d_{LZ} - (d_{LZ} - Z)}{2[D_1(t - t_{n+1})]^{1/2}} \right] + \operatorname{ierfc} \left[\frac{(2m-1)d_{LZ} + (d_{LZ} - Z)}{2[D_1(t - t_{n+1})]^{1/2}} \right] \right\} \end{aligned} \quad (1)$$

where d_{LZ} is the thickness of the permeable soil layer, K_S is the saturated hydraulic conductivity, $\beta = \cos^2 \delta$, δ is the terrain slope, $H(\bullet)$ is the Heaviside step function, $D_1 = D_0 / \cos^2 \delta$, D_0 being the saturated soil diffusivity, and $\operatorname{ierfc}(x) = \frac{1}{\sqrt{\pi}} \exp(-x^2) - \operatorname{erfc}(x)$, erfc being the complementary error function. Pressure head under

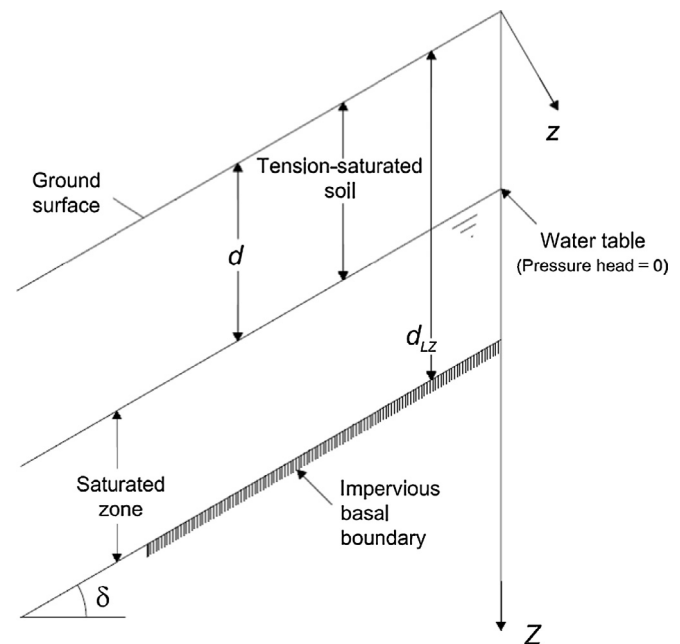


Fig. 1. Sketch illustrating the TRIGRS model for pore pressure head and slope stability computation (adapted from Baum et al., 2002).

downward gravity-driven flow cannot exceed that resulting when the water table is at the ground surface (Iverson, 2000), namely:

$$\psi(Z, t) \leq Z\beta \quad (2)$$

One of the main assumption of the model is that the solution presented in Eq. (1) is valid only for tension-saturated initial conditions, so that a linearized version of the Richards' equation can be considered to be valid, and the hydraulic conductivity can be approximated by its value at saturation (Iverson, 2000; Baum et al., 2010). It is worth to mention that in our application, no flow routing due to rainfall exceeding infiltration capacity is performed.

After pressure head is computed according to Eqns. (1–2), the factor of safety, which measures the degree of geomechanical stability is computed by the infinite slope formula (Taylor, 1948):

$$FS(d_{LZ}, t) = \frac{\tan \phi'}{\tan \delta} + \frac{c' - \psi(d_{LZ}, t)\gamma_w \tan \phi'}{\gamma_s d_{LZ} \sin \delta \cos \delta}, \quad (3)$$

where c' is soil cohesion for effective stress, ϕ' is the soil friction angle for effective stress, γ_w is the unit weight of groundwater, γ_s is the soil unit weight. In the scheme associated with Eq. 3 the

failure occurs at the basal boundary, $Z = d_{LZ}$, since pressure head results maximum at that depth.

2.2. Debris flow propagation model

FLO-2D is a commercial code developed by O'Brien (1986), adopted worldwide for modeling debris flow phenomena and delineating flood susceptibility. It is a pseudo two-dimensional model in space, based on depth-integrated flow equations. Hyper-concentrated sediment flows are simulated considering a mono-phase approach, assuming an empirical quadratic rheological relation (O'Brien, 1986). The basic equations implemented in the model consist of the continuity equation:

$$\frac{\partial h}{\partial t} + \frac{\partial(hV)}{\partial x} = i \quad (4)$$

and the equation of motion:

$$S_f = S_o - \frac{\partial h}{\partial x} - \frac{V}{g} \frac{\partial V}{\partial x} - \frac{1}{g} \frac{\partial V}{\partial t} \quad (5)$$

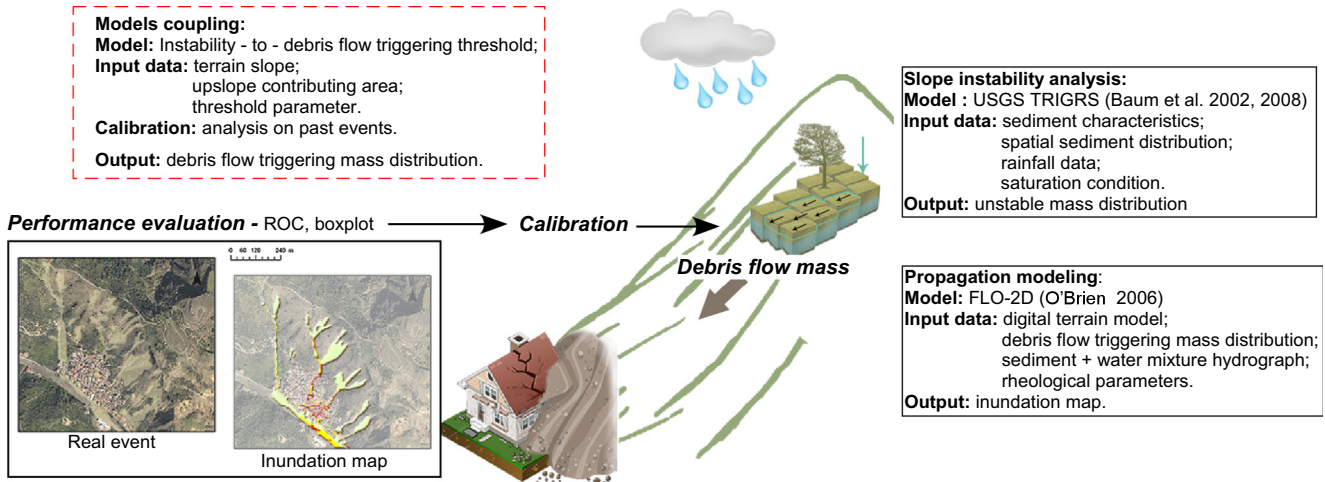


Fig. 2. Representative sketch of the different steps and related input data that characterize the proposed methodology.

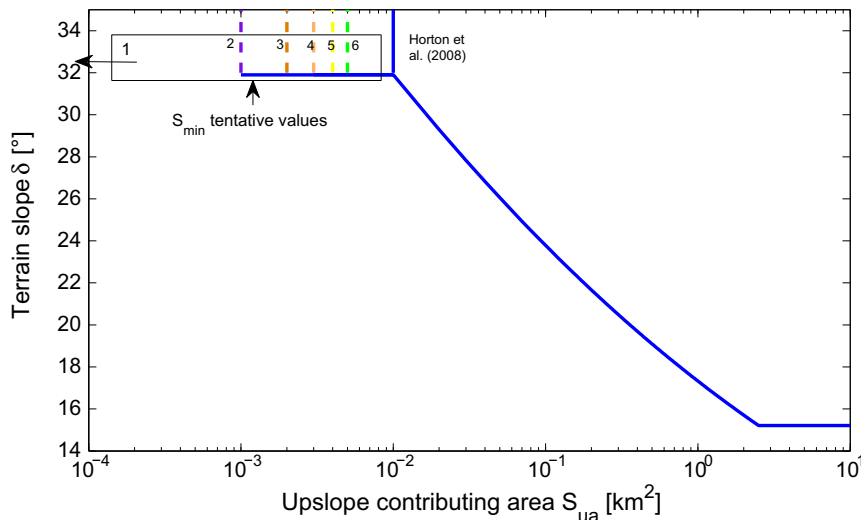


Fig. 3. Threshold for deriving debris flow propagating cells from the unstable ones, determined via the TRIGRS Grid-Based Infiltration and Slope stability model. The S_{min} parameter is to be calibrated, based on comparison with observed debris flow inundation maps and ROC analysis. The values corresponding to the six simulations performed later in Section 3.3 are also indicated in the plot.

where S_o is bed slope, h is the flow depth, V is the depth-averaged velocity, i is the excess rainfall intensity (assumed equal to zero in the present application), and x is the generic direction of motion.

In order to solve the momentum equation, FLO-2D considers, for each cell, eight potential flow directions. Each velocity computation is essentially one-dimensional and solved independently from the other seven directions, so h and V are related to one of the eight flow directions x .

The total friction slope can be expressed as follows:

$$S_f = \frac{\tau_B}{\rho gh} + \frac{K\mu_B V}{8\rho gh^2} + \frac{n^2 V^2}{h^3} \quad (6)$$

where τ_B is the Bingham yield stress, h is the flow depth, V is the mean flow velocity along the flow direction, ρ is mixture density, K is the laminar flow resistance coefficient, g is gravitational acceleration, μ_B is the Bingham viscosity, and n is the pseudo-Manning's resistance coefficient, which accounts for both turbulent boundary friction and internal collisional stresses. In particular, the yield stress τ_B , the dynamic viscosity μ_B and the resistance coefficient n are influenced by the sediment concentration and, therefore, can be described by the following equations (O'Brien, 2006):

$$\tau_B = \alpha_1 e^{\beta_1 C_v} \quad (7)$$

$$\mu_B = \alpha_2 e^{\beta_2 C_v} \quad (8)$$

$$n = n_t 0.538 e^{6.0896 C_v} \quad (9)$$

where C_v is the volumetric concentration, $\alpha_1, \beta_1, \alpha_2$ and β_2 are empirical coefficients defined by laboratory experiments (O'Brien

and Julien, 1988, and n_t is the turbulent n-value (O'Brien, 2006). More detailed information about the numerical scheme and the general constitutive fluid equations adopted in the model can be found in O'Brien (2006).

2.3. Models coupling

The proposed procedure for coupling the hydrological and propagation models can be described following the sketch illustrated in Fig. 2, where the different modelling phases and the related input data are presented.

As already mentioned, a key step of the procedure is the identification of the triggering cells, to be applied as input to the propagation model, among the potentially unstable ones identified through the slope instability analysis. Indeed, such a step is crucial for a proper mass release simulation (Lehmann and Or, 2012), since generally not all the unstable cells move downward as a debris flow. Within the proposed approach the slope stability model is linked to the propagation model by applying a triggering-to-debris flow instability threshold. In particular, once the triggering rainfall event is defined and the soil moisture initial conditions are defined, the cells potentially unstable are computed as those characterized by a factor of safety less than 1 ($FS \leq 1$), thus obtaining the map of potentially unstable cells. Such cells then may take part to two different possible instability triggering phenomena (see Marchi et al. (2002): a) hyper-concentrated flow, b) debris flow generation. The instability-to-debris flow triggering threshold aims at distinguishing the triggering volume involved in these two processes. The unstable cells whose characteristics fall above the threshold propagate as a debris flow, while those below contribute to hyper-concentrated flow. Only the cell that contribute

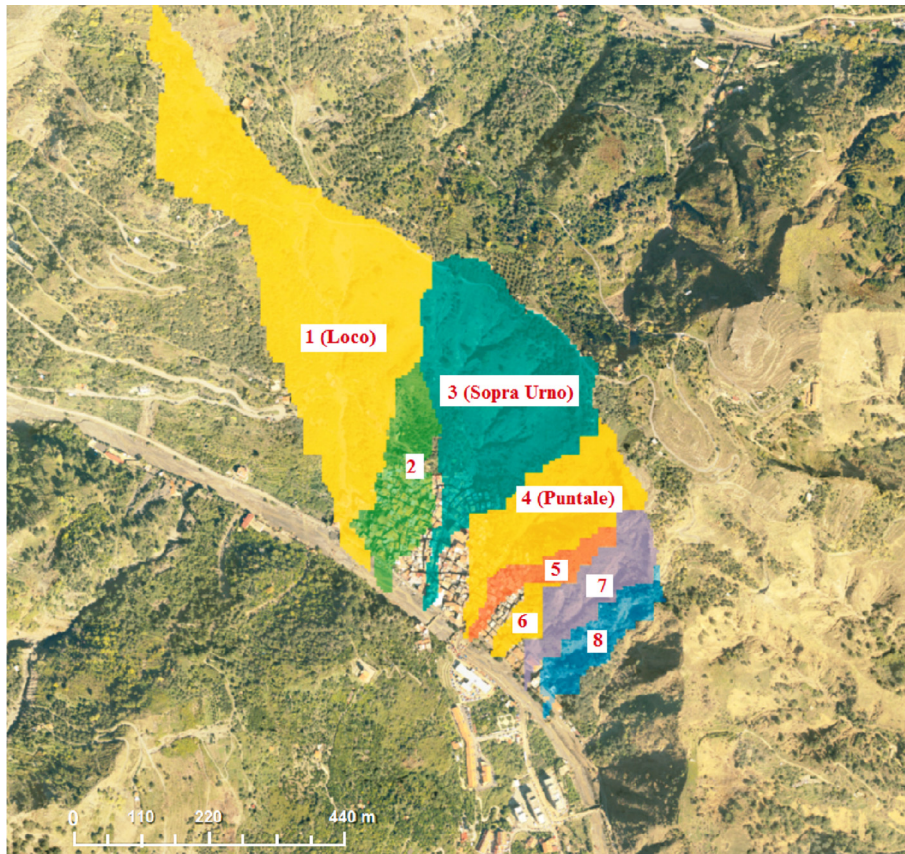


Fig. 4. Map showing the creek basins in the analysed area, where basins are numbered from left to right. Nomenclature follows the scientific literature (Peres and Cancelliere, 2016; Stancanelli et al., 2014; Stancanelli and Foti, 2015).

to debris flow formation are inputted to the debris flow routing model (FLO-2D in our case).

In general, whether or not a cell is triggered depends on the sediment characteristics (i.e. mean grain size, permeability, cohesion, etc.) and sediment spatial distribution (i.e. soil depth variation), as well as the geological characteristics of the catchment (i.e. terrain slope) (Takahashi, 1981). For an area of given soil properties, the main variables controlling the transition between instability and landslide triggering, are terrain slope δ and the upslope contributing area S_{ua} (Rickenmann and Zimmermann, 1993; Horton et al., 2013; Park et al., 2013; Blahut et al., 2010).

In our work, we slightly modify the instability-to-debris flow triggering threshold for terrain slope δ proposed by Rickenmann and Zimmermann (1993) and others (Horton et al., 2013; Park et al., 2013; Blahut et al., 2010), for extreme debris flow events:

$$\tan \delta = \begin{cases} 0.312S_{ua} & \text{if } 0.01\text{km}^2 \leq S_{ua} < 2.5\text{ km}^2 \\ 0.26 & \text{if } S_{ua} \geq 2.5\text{ km}^2 \end{cases} \quad (10)$$

where S_{ua} is the upslope contributing area and δ the terrain slope.

The instability-to-debris flow triggering threshold may be derived by analysing several debris flow events occurred in a specific area. Here we introduce a parameter in Eq. 10 to be calibrated based on observations of real debris flow event, maintaining the same functional form. We choose to have just one free parameter since this leads to higher generalization capabilities as well as simplicity. In particular, in the above mentioned studies the most uncertain parameter seems to be the minimum contributing area for initiation. Thus, in order to adapt such instability-to-debris flow triggering threshold in basins characterized by a relatively small area (approximately less than 1 km^2), we propose the following threshold:

$$\tan \delta = \begin{cases} 0.618 & \text{if } S_{min} \leq S_{ua} < 0.01\text{ km}^2 \\ 0.312S_{ua}^{-0.15} & \text{if } 0.01\text{ km}^2 \leq S_{ua} < 2.5\text{ km}^2 \\ 0.26 & \text{if } S_{ua} \geq 2.5\text{ km}^2 \end{cases} \quad (11)$$

where the minimum contributing area S_{min} is calibrated on the basis of observed events (see Figs. 2 and 3).

The calibration of S_{min} is carried out by searching the value which leads to the best reproduction of the observed debris-flow propagation and deposition. To this end, Receiver Operating Characteristic (ROC) analysis is used to compare the performances of the model for different values of S_{min} . The optimal S_{min} value can then be potentially used as a reference value for a predictive susceptibility mapping in similar regions, namely in an area characterized by similar geology and rainfall climate. Various ROC indexes can be used to measure the model performance (Frattini et al., 2010). Suitable indexes are the Equitable Critical Success Index (ECSI), also known as the Equitable Threat Score or Gilbert skill score, and the Heidke skill score (HSS). These indexes are defined as:

$$ECSI = \frac{TP - TP_{rnd}}{TP + FN + FP - TP_{rnd}} \quad (12)$$

$$HSS = \frac{TP + TN - E}{T - E} \quad (13)$$

where TP is the number of true positives, FN the number of false negatives, FP the number of false positive, $T = TP + FN + FP + TN$, $TP_{rnd} = \frac{(TP+FN)(TP+FP)}{T}$ and $E = \frac{1}{T}(TP + FN)(TP + FP) + (TN + FN)(TN + FP)$. In our case, TP is the number of cells where the debris material has deposited both in the field and in simulation; TN is the number of cells where the debris material has not deposited both in the field and in simulation; FP is the number of cells where



Fig. 5. Photo-panorama of Giampilieri village after the alluvial event: a) the slope scoured by debris flows; b) Giampilieri urbanized area damaged by the alluvial event; c) Giampilieri urbanized area where the sediment deposit level is recognizable.

the debris material has deposited in the simulation but not in the field; FN is the number of cells where the debris material has deposited in the field but not in simulation. The two chosen indexes seems to be among those that suffer less about the limitations of other indexes when the goal is the reproduction of spatial information where the number of Negatives is much higher than the number of Positives, such as in landslide phenomena (Murphy, 1996; Frattini et al., 2010).

3. Application

3.1. Case study area

The analysed area is located in the Peloritani mountains, Sicily, Italy. Specifically we consider debris flow data from the event of 1 October 2009 that hit the town of Giampilieri. Giampilieri is a small village located in the South part of Messina Province (Sicily). The historic and most urbanized part of the town is located on the left bank of the Giampilieri river and is mainly settled on slopland, because of the limited plain area available and the peculiar geomorphologic conditions of the site. The town is crossed by three

main tributaries of the Giampilieri river (from West to East: Loco, Sopra Urno and Puntale streams) and others smaller catchments (indicated in Fig. 4 with a reference number). The three main streams drain small watersheds of 0.14 km² (Loco), 0.07 km² (Sopra Urno) and 0.03 km² (Puntale) characterized by narrow valleys (Fig. 4), with elevation ranging approximately between 50 and 400 m a.s.l., and with a significant proportion of slopes in the interval 30°–40°. Soil in the area is composed by highly erodible metamorphic material. The pluviometric regime is that typical of the semiarid areas, with long dry spells during the summer, and high intensity rainstorms of short duration occurring mostly between October and March. The morphology of the small catchments leads to impulsive flash-flood responses. The Peloritani Mountains in general are shaped as several gullies next to each other which induce a high rainfall spatial variability due to orographic effects.

On 1 October 2009, about 250 mm of rainfall fell in 9 h, which triggered more than 600 landslides, in an area of 50 km² of the Messina Province, mostly evolving into devastating debris flows. This event caused the death of 37 persons, about 100 injuries and the evacuation of 1700 residents (Foti et al., 2013).

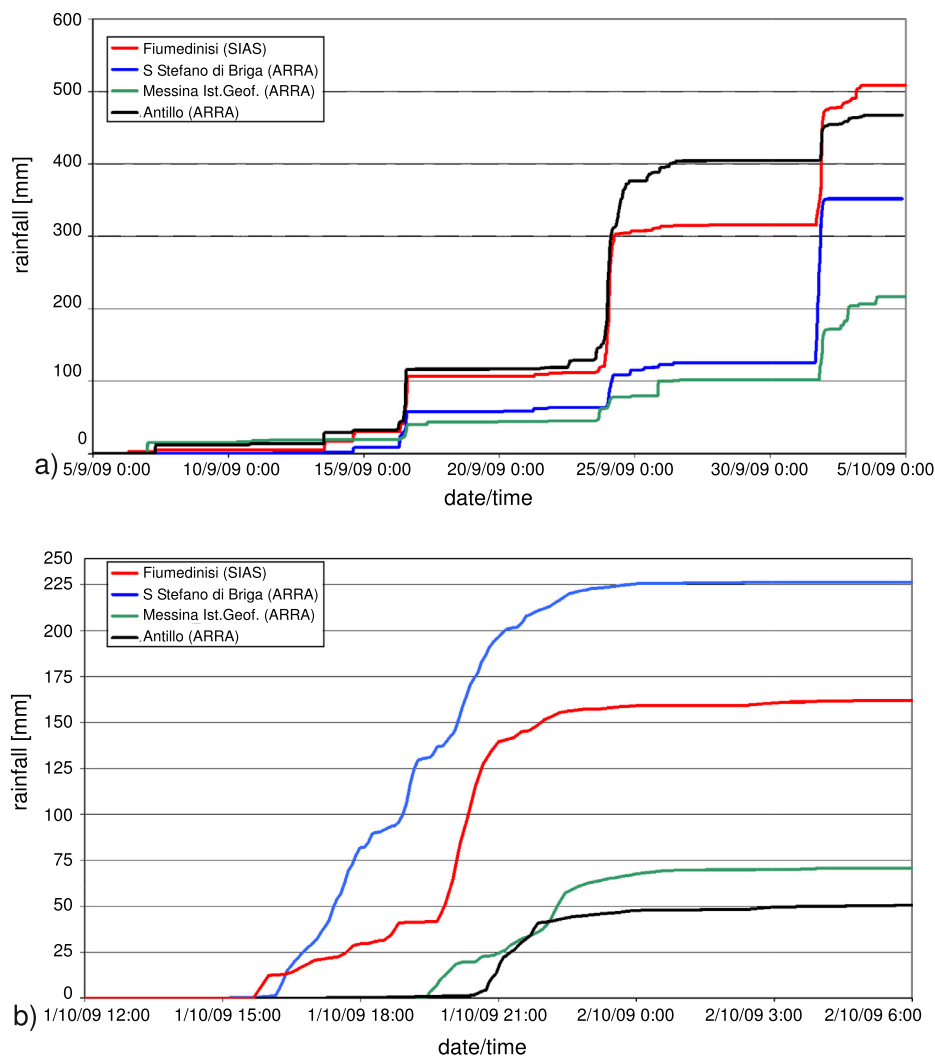


Fig. 6. Cumulative rainfall depth data reconstructed from information coming from Fiumedinisi, S. Stefano di Briga, Messina Istituto Geofisico and Antillo stations, for the period ranging: a) from 5th September to 5th October 2009; b) from 12:00 of 1st October 2009 until 6:00 a.m. of 2nd October 2009.

Fig. 5 shows evidences about slope erosion (see Fig. 5a) and damages occurred to the Giampilieri village (Fig. 5b and c).

Return period of the rainfall event has been estimated based on observations from the rain gauges in the nearby area in the order of hundreds of years (Foti et al., 2013). Although landslide triggering may occur for lower return periods (Schilirò et al., 2015), the exceptional magnitude of the event may be also related to a high 15-days antecedent cumulative precipitation, greater than 100 mm, according to measurements of the rain gauge station nearest to Giampilieri in S. Stefano di Briga (see Fig. 6a).

Cumulative rainfall depths in the period September 5th–October 5th, 2009 are shown in the Fig. 6a. Such rainfall data were collected by four different stations (Fiumedimisi, S. Stefano di Briga, Messina Istituto Geofisico, Antillo). The Messina Province has been affected by three important rainfall events, occurred on 16th September 2009, 23rd–24th September 2009 and 1st October 2009. Therefore, the 1st October event it can be assumed that happened when the soil was close to saturated condition. Fig. 6b shows a detailed representation of rainfall the event of October, 1st 2009 by means of the data gathered from rain gauges, showing the high spatial variability of the rainfall event.

The analysis of post event conditions provide useful information about the event development and the consequent damages. Debris flow propagation path presented in Fig. 7 affected both the natural slopeland area (defined in the legend as basin) and the urbanized area. Such a distinction will be useful later on for

discussing results. Data on sediment deposit level inside the urbanized area are also available (see Fig. 7b)). This reference map reflects propagation of only debris flow material, and not that of hyperconcentrated flows. Indeed, the latter component is assumed to exit the area under investigation, because of its relatively low viscosity.

3.2. Input data

The topographic input consist of a digital terrain model (DTM) acquired before the alluvial event of 2009 and characterized by a resolution of 2 m. The DTM has been integrated with information from official maps and orthophotos, concerning the distribution of the buildings. A grid system, with square cells 2×2 m, has been used as a base for modeling processing. Soil properties data used to compute unstable cells by means of the TRIGRS model, and globally representative of the Giampilieri area, are summarized in Table 1. Most of the properties are assumed to be constant within the basin, except for soil depth, which has been related to slope using a relationship calibrated on available borehole measurements $d_{lz} = 32 \exp(-0.07\delta)$ (Peres and Cancelliere, 2016). The limited knowledge of soil proprieties distribution is a problem common to many studies (Montgomery and Dietrich, 1994; Borga et al., 2002; Rosso et al., 2006; Salciarini et al., 2008; Baum et al., 2010; Tarolli et al., 2011), which explains why constant sediment characteristic along the soil depth are generally assumed in

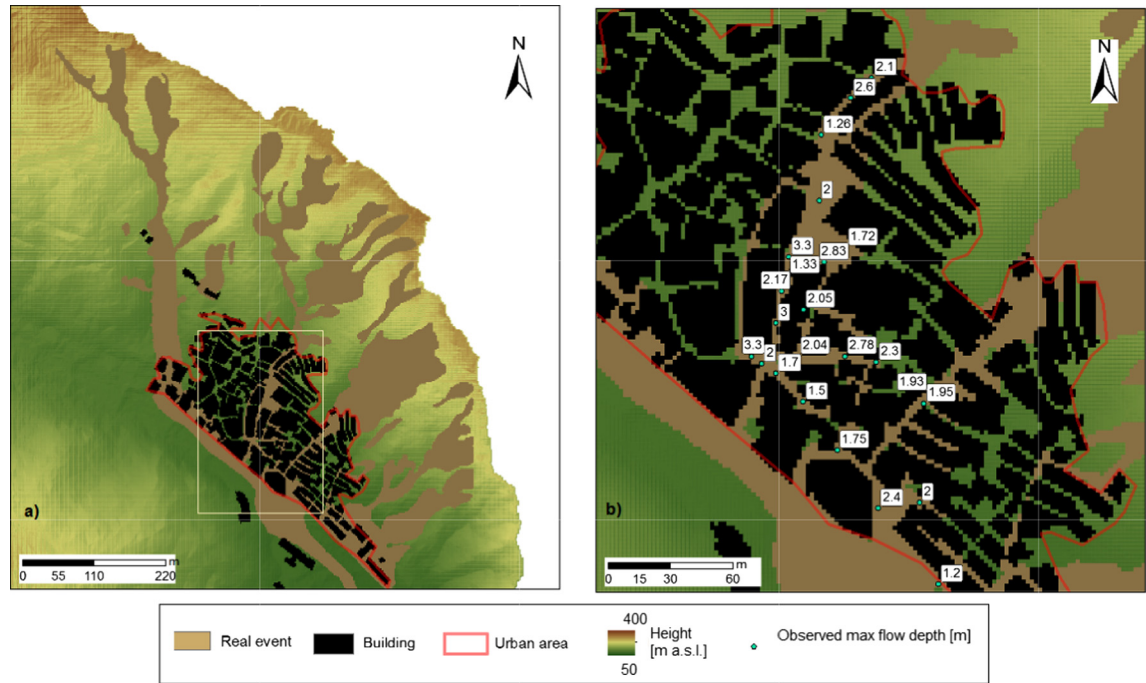


Fig. 7. 1 October 2009 maps showing the assumed real event data for model calibration and performance assessment: a) areas affected by landslide-debris-flow phenomena, b) enlargement showing locations and values of observed maximum flow depths in the urbanized area of Giampilieri village. Maps show the urban area considered in performance assessment for comparison of the performances in such area respect to those on the whole area.

Table 1
Soil properties data used as input to the TRIGRS model (Peres and Cancelliere, 2016).

ϕ' [°]	c' [Pa]	γ_s [N/m ²]	K_s [m/s ²]	D_0 [m ² /s]	d_{lz} [m]
39	4000	19000	2×10^{-5}	5×10^{-5}	$32 \exp(-0.07\delta)$

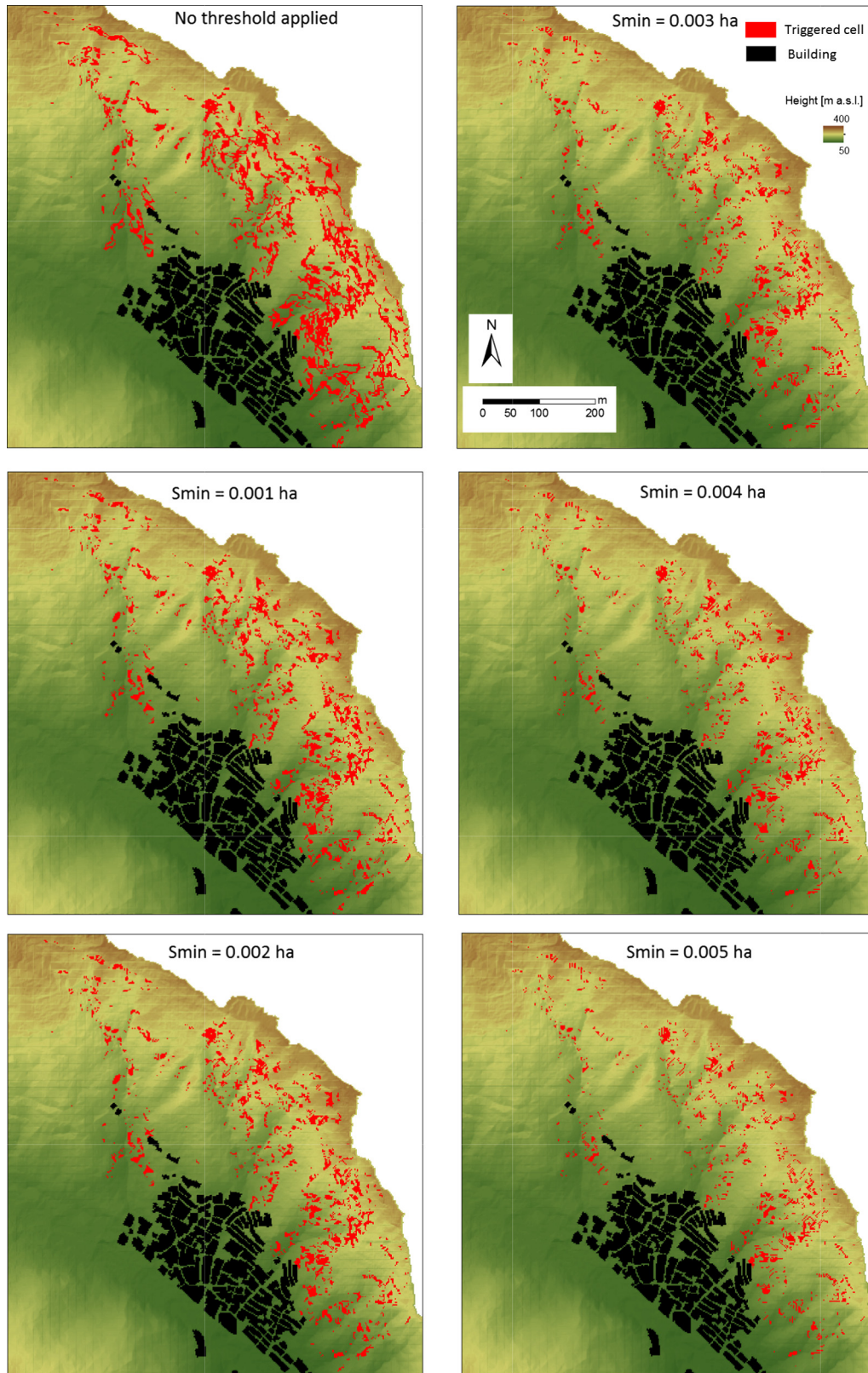


Fig. 8. Maps showing the simulated triggered cells for the 1 October 2009 event, obtained by the TRIGRS model and subsequent application of the instability-to-debris-flow-triggering threshold with different values of the S_{min} parameter, as indicated in the panels. Simulations have been carried out considering as input to the TRIGRS model the hourly-resolution rainfall event measured at the nearest raingauge available (S. Stefano di Briga).

practice. This limit hampers the application of more sophisticated models based on distributed hydrological variables (as soil moisture, lateral water flow, infiltration, streamflow), as the one

proposed recently by [Anagnostopoulos et al. \(2015\)](#), which includes also analysis of phenomena as solid hydraulic hysteresis and preferential flow, increasing model predictive capability. [Fan](#)

et al. (2016), based on the application of a stochastic approach to model the triggering phenomena using soil type and initial water content variation data, indicates that the soil propriety variability could be responsible of an increase of landslide volume. It is worth to point out that among all soil proprieties the spatial distribution of sediment characteristics plays a crucial role on the model predictive ability (Lanni et al., 2013; Brönnimann et al., 2013; Anagnostopoulos et al., 2015). Nevertheless, the modeling of soil parameter uncertainties falls beyond the scope of this paper.

Regarding the hydraulic condition, the rainfall time history in different stations back to one month up to the 1 October rainfall event shows a significant amount of antecedent rainfall (see Fig. 6a). This likely allows the use of a tension-saturated model for simulating infiltration processes triggering landslides on 1 October 2009 (see Section 2.1). In general, a more precise infiltration model is needed to account for infiltration dynamics in the unsaturated zone considering the soil water characteristic curve, and thus a less simplified version of the Richards' equation (see e.g. Baum et al., 2008; Baum et al., 2010; Peres and Cancelliere, 2014; Peres and Cancelliere, 2016). Considering that the rainfall alluvial event was characterized by high spatial variability, our application has been carried out by using the data of Santo Stefano di Briga rainfall gauge station (see Fig. 6b), which is the closest to the investigated area and therefore it is considered representative of the 1 October 2009 event in Giampilieri (Peres and Cancelliere, 2014). This rainfall time series has been inputted to the TRIGRS model at an hourly time step. The final instability map corresponding to few hours after the cease of rainfall is used in input to the propagation model FLO-2D, after applying the instability-to-debris-flow-triggering threshold.

Regarding the calibration of the triggering to debris flow threshold (see Eq. 11), the debris flow susceptibility maps are obtained considering the total amount of unstable volume defined by the rainfall infiltration and geotechnical instability model, and then those resulting applying Eq. 11 with the following values of the triggering parameter S_{min} are assumed: 0.001 ha, 0.002 ha, 0.003 ha, 0.004 ha, 0.005 ha.

Regarding the propagation model, the debris flow phenomena is simulated considering the unstable volume in each grid cell. In light of the soil saturated condition, each single unstable cell volume is transformed in a water–sediment mixture triangular hydrograph characterized by a sediment concentration of 0.5, with time peak equals to the average basin concentration time (about 6 min). The unstable cells are modeled to be triggered as debris flow at the same instant, the effects of delayed mass release being beyond the scope of this paper. The rheological characteristics of the propagating mixture, such as the yield stress τ_B , the dynamic viscosity μ_B and the resistance coefficient n , are those determined by Stancanelli and Foti (2015), which were obtained through a calibration procedure carried out with reference to the same area considered in this study.

3.3. Debris flow susceptibility assessment

Debris flow susceptibility assessment is carried out applying the proposed methodology (indicated in the following as SD “spatially distributed” input) to the Giampilieri area where data of the 1 October 2009 event, described in Section 3.2, are available for calibration and validation.

First, we carried out the slope instability analysis by means of rainfall infiltration and geotechnical instability model (Section 2.1). Fig. 8 shows the results in terms of instability map applying the TRIGRS model, and considering the six different values of the S_{min} parameter in Eqn. 11.

From the first instability map of the Fig. 8, the presence of isolated unstable cells can be seen. This is related to the infinite slope assumption in the adopted geotechnical model, for which the failure of each cell is assumed to be independent from the other ones in the catchment. Due to lateral (parallel to the hillslope) forces, real failure generally presents some connectivity, a feature which is better captured by models which include a multi-dimensional analysis of failure (cf. Lehmann and Or, 2012; Milledge et al., 2014; Bellugi et al., 2015; Anagnostopoulos et al., 2015), to which our approach may be potentially extended.

The values of S_{min} adopted in the simulations and the resulting triggered volumes are reported in Table 2. In case of lower and higher S_{min} the debris flow volume is assumed to have a reduction respectively of 34% and 67% of the total triggering volume ($S_{min} = 0$).

The landslide-triggering maps are used directly as input to the FLO-2D propagation model; specifically, a hydrograph of volume equal to that of the displaced soil, is associated to each triggered cell. The inundated areas thus obtained by means of the propagation model are shown in Fig. 9.

The extent of inundation area and the flow-depths (see Fig. 9) at the end of the event decreases as higher values of the triggering threshold S_{min} are applied to the slope instability map.

A few other simulations, emulating the usual procedure of modeling debris flow run-out with the total unstable volumes of debris mixture hydrographs triggered at the top of the sub-basin streams, have also been carried out. We refer to this method as the “traditional” T one. The aim is to have a reference useful for evaluating the performance of the SD approach proposed here. In particular SD simulations adopted for comparison are those performed with the volumes resulting from the application of the less restricting thresholds, corresponding to lower values of S_{min} (case of no threshold, then $S_{min} = 0.001$ ha and $S_{min} = 0.002$ ha). The resulting inundation maps are presented in Fig. 10.

The spatial distribution of the cells affected by debris flows resulting from the different scenarios is evaluated by comparison with the observed inundation maps, based on the ROC-based indexes of Eqs. 12 and 13 (as shown in Fig. 11).

The performances have been assessed separately for the whole domain of simulation (denoted as “basin”) and for the urbanized area (indicated as “urban”), which are defined in Fig. 7a.

Table 2

Input triggered volumes, computed by TRIGRS and the specified unstable-to-triggering threshold, for each considered basin (see Fig. 5a). These volumes have been used as input in the traditional hydrograph-based approach.

	Volume per basin [m ³]								
	1 (Loco)	2	3 (Sopra Urno)	4 (Puntale)	5	6	7	8	Total
TRIGRS as-it-is	11060.8	57.9	20769.6	13814.9	1635.4	319.4	5888.3	3969.2	57515.5
$S_{min} = 0.001$ ha	7662.1	50.3	14272.5	9452.1	1076.8	242.9	3182.6	2273.0	38212.2
$S_{min} = 0.002$ ha	6513.4	42.8	12383.2	8431.8	946.9	188.5	2623.9	1937.2	33067.7
$S_{min} = 0.003$ ha	5055.0	29.2	9919.2	7142.5	770.9	101.4	2053.9	1508	26580.2
$S_{min} = 0.004$ ha	4191.0	15.3	8540.7	6459.5	684.9	81.2	1817.3	1302.6	23092.4
$S_{min} = 0.005$ ha	3354.8	15.3	6944.6	5649.6	547.3	40.3	1489.3	1105.5	19146.7

As it can be inferred from the plots, there is a significant difference between the quality of the reproduction of the real event related to the whole basin (indicated in black within the figure) and that related to the urbanized area only (red lines), where the

model clearly performs better. This highlights that the prediction of triggered areas is a difficult task; in the urban area results are better, but there clearly large margins of improvement (ROC indexes are not higher than 0.8). Lower assessment performance,

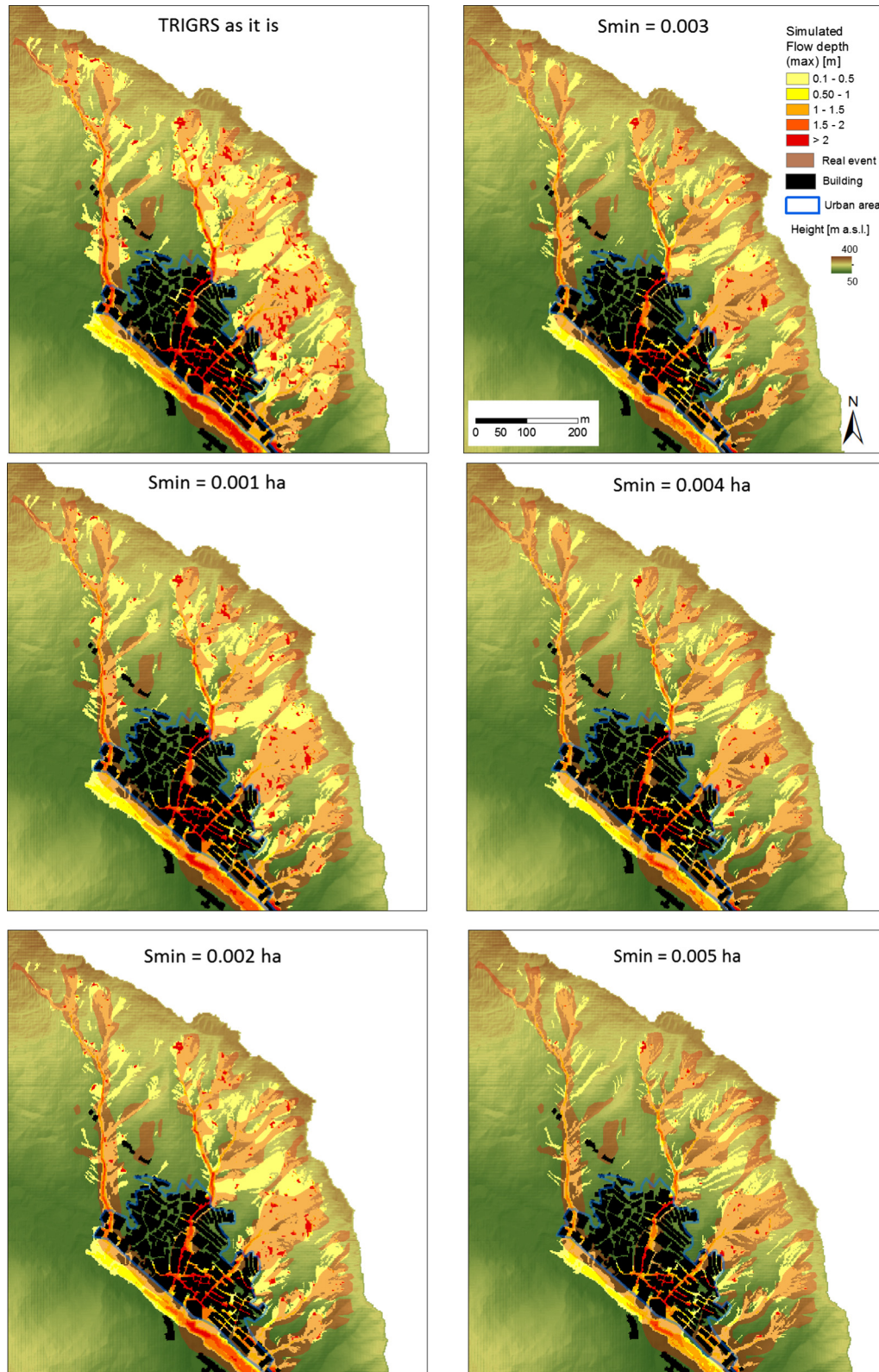


Fig. 9. Estimated inundation maps corresponding to different instability-to-debris flow triggering thresholds (Spatially Distributed input: SD).

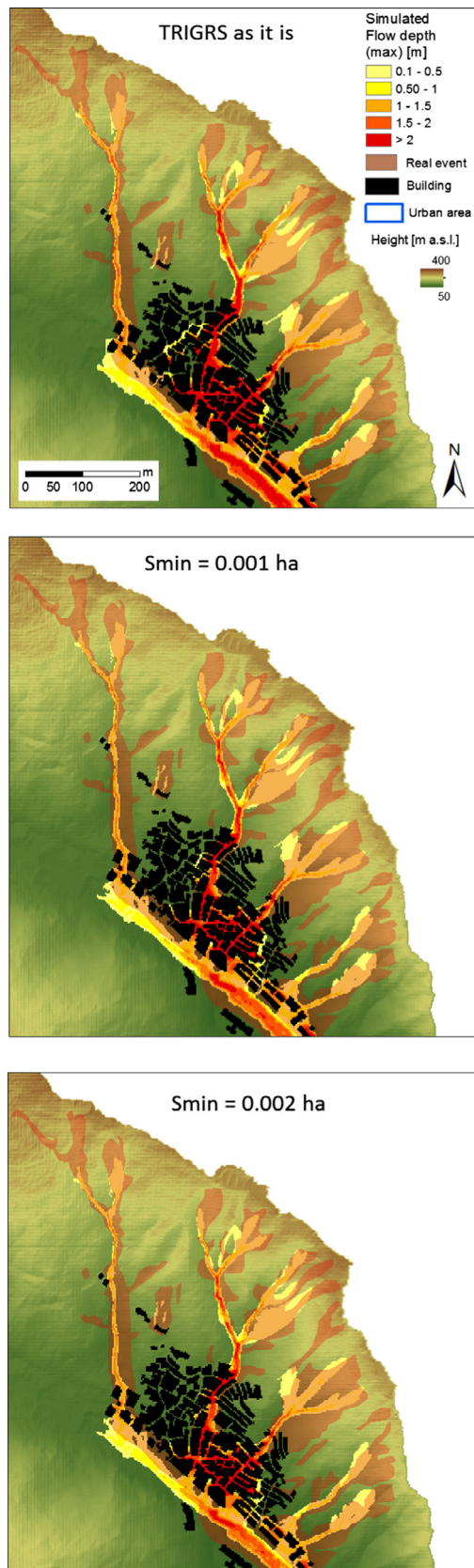


Fig. 10. Estimated inundation maps corresponding to different instability-to-debris flow triggering thresholds where inputs are given as lumped hydrographs (Traditional input: T).

in case of the entire area, is presumably addressable to assumption of constant sediment characteristics within the basin. Indeed, the latter influences the evaluation of the triggering volume and its distribution on the slopes (basin area). On the other hand, better performance results are obtained within the urbanized area, where factors as DEM accuracy (high in our case) and rheological parameters (previous calibrated in [Stancanelli and Foti \(2015\)](#)) play a significant role.

From [Fig. 11](#), it can be inferred that performances of the SD and T approaches are very similar with respect to the urban area (see red continuous and dotted lines), while with respect to the whole basin area, the former performs significantly better. This reflects the fact that triggered areas are taken into account when specifically assessed by suited models, whereas they are neglected in the case of the traditional hydrograph-based approach. Indeed the better results obtained by the T approach in the urbanized area are partially due to the reduced heterogeneity and the presence of roads and buildings that limit the possible flow paths.

Regarding the best value of the threshold parameter S_{min} it can be seen that the differences are quite small, but still it seems that performances decrease as the threshold parameter S_{min} becomes more restrictive, though it can be stated that the first three simulations are practically equivalent in terms of resulting ROC indexes. In order to better identify which of the three simulations is the best, a comparison between observed and simulated depths at the same point locations has been performed (see [Fig. 7](#)); [Table 3](#) shows the related data.

Direct comparison of such depths may not be particularly significant, since it depends on the criteria by which the comparison is carried out. Hence we consider more adequate a coarser assessment, based on the global distribution of debris flow depths in the observation locations, with the aim is to understand if the model performs globally well in reproducing the magnitudes of the flow depths. The box-plots of [Fig. 12](#) compare the distribution of maximum flow depths, as derived from [Table 3](#).

In particular, for each value of S_{min} the first box-plots represent the distribution of observed maximum flow-depths on the points where observations were available, and the second one represents that of the simulated flow-depths. As it can be seen from the box-plots, to apply no instability-to-debris flow triggering filter leads to an over-estimation of the flow-depths. This may be accepted in some applications, if one desires conservativeness of results. Filter of $S_{min} = 0.001$ ha leads indeed to the best results, since $S_{min} = 0.002$ ha is not conservative in this case the median maximum flow-depth, represented by central line of the box plots, is less than the observed median.

The results allow to state that for a susceptibility assessment at the catchment scale the SD approach may be more reliable and conservative, while, in the case that one needs to assess susceptibility in the urbanized area, the traditional approach may still yield reliable results.

Finally, in order to evaluate the performance of the rainfall infiltration and geotechnical instability model in estimating the total eroded volume from the slope and the feasibility of the triggering to debris flow threshold application, the unstable volume have been estimated by commonly-applied empirical formulas and then compared them to those obtained with our methodology (see [Table 2](#)). [Table 4](#) shows unstable volume estimation for the Loco basin determined applying different approaches, such as: comparison of pre and post event Digital Terrain Model (DTM) ([Ventisette et al., 2012](#)), output of the TRIGRS modelling, empirical formulations ([Bianco and Franzi, 2000](#); [Bottino et al., 1996](#); [Kronfellner-](#)

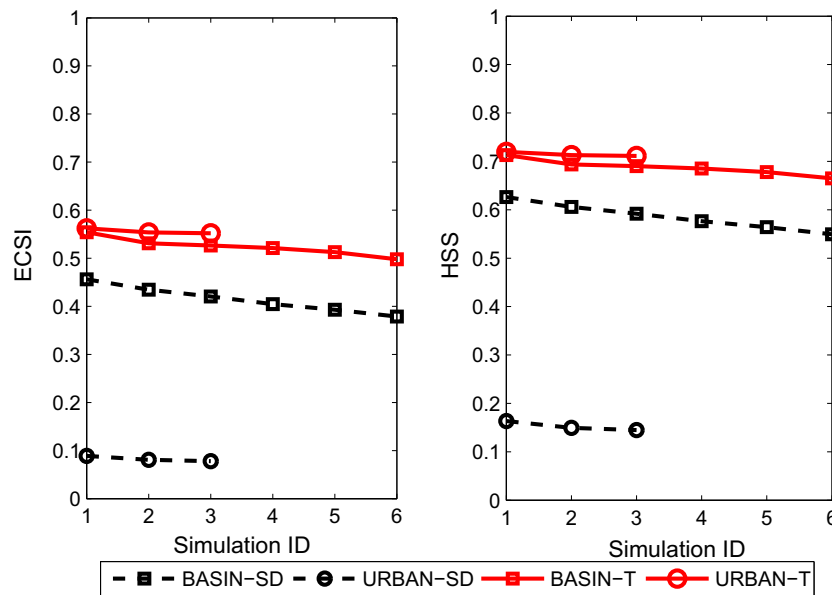


Fig. 11. Assessment of model performances in the areal reproduction of the real 1 October event for all six values of the parameter S_{min} in terms of the Equitable Critical Success Index (ECSI) and the Heidke skill score ROC indexes represented for the basin area and the urbanized area, for the proposed spatially-distributed (SD), and the traditional (T) methodologies. The SIMULATION IDs represent respectively the following: 1. “No threshold”, 2. $S_{min} = 0.001$ ha, 3. $S_{min} = 0.002$ ha, 4. $S_{min} = 0.003$ ha, 5. $S_{min} = 0.004$ ha, 6. $S_{min} = 0.005$ ha. Though the indexes exhibit only little variations respect to S_{min} , there is a clear difference between performances in the urban area and those in the whole simulation domain. In particular performances in the whole basin are worse than those in the urban area.

Table 3

Comparison of maximum flow depths [m] measured and simulated at the specific locations shown in Fig. 7, for both the proposed (spatially distributed) and traditional methodologies.

Observed	Spatially distributed method			Traditional method		
	$S_{min} = 0.001$ ha	$S_{min} = 0.002$ ha	$S_{min} = 0.003$ ha	$S_{min} = 0.001$ ha	$S_{min} = 0.002$ ha	$S_{min} = 0.003$ ha
3.30	1.94	1.86	1.74	2.89	2.17	1.96
2.00	1.88	1.80	1.68	2.83	2.11	1.89
3.00	5.15	5.02	4.75	6.63	5.76	5.46
1.70	2.11	1.96	1.67	3.16	2.41	2.17
2.17	5.53	5.32	4.91	7.46	6.30	5.96
3.30	3.82	3.65	3.33	5.58	4.52	4.12
2.04	1.58	1.44	1.20	2.55	1.90	1.69
1.33	2.64	2.47	2.17	4.37	3.32	2.97
2.05	0.00	0.00	0.00	0.00	0.00	0.00
1.50	3.08	2.81	2.35	4.90	3.70	3.29
1.26	2.10	2.00	1.81	3.10	2.50	2.29
2.00	1.71	1.63	1.50	2.44	1.97	1.82
2.83	1.50	1.33	1.02	3.20	2.13	1.76
1.75	1.88	1.69	1.46	3.07	2.28	2.02
1.72	0.00	0.00	0.00	0.93	0.00	0.00
2.78	2.60	2.46	2.21	3.61	2.99	2.74
2.60	4.32	4.14	3.83	6.13	5.09	4.71
2.10	3.48	3.27	2.94	5.72	4.55	4.13
2.30	2.65	2.49	2.23	3.67	3.01	2.81
2.40	1.27	1.17	1.07	1.93	1.52	1.38
2.00	1.12	1.02	0.90	1.77	1.36	1.22
1.95	1.56	1.51	1.37	3.13	2.45	2.25
1.93	1.53	1.50	1.40	2.78	2.23	2.08
1.20	0.27	0.27	0.23	0.36	0.32	0.31

Kraus, 1984; Marchi and Tecca, 1996; Tropeano and Turconi, 1999). It is quite evident that the empirical formulations give only approximate estimations of the possible maximum intensity of slope erodible events (Kritikos and Davies, 2014) and present an high variability. In any case, the results obtained by the proposed methodology suggest that the estimation performed by Ventisette et al. (2012) is comparable in dimension $O(10^4 m^3)$ with the one evaluated by means of the physically based slope stability model, when no instability-to-debris flow triggering threshold is

applied. The application of the instability-to-debris flow triggering threshold is useful to identify the portion of the total unstable sediment that concurs to the debris flow formation. In case of the alluvial event of 1 October 2009 for the Loco basin, the best simulation (see $S_{min} = 0.001$ ha in Table 2) indicates that an amount of about 31% of the total sediment unstable volume is eroded as hyperconcentrated flow phenomena. That means that the debris flow that is preceded by a 30 min of hyperconcentrated flow, when assuming a solid concentration of 0.2.

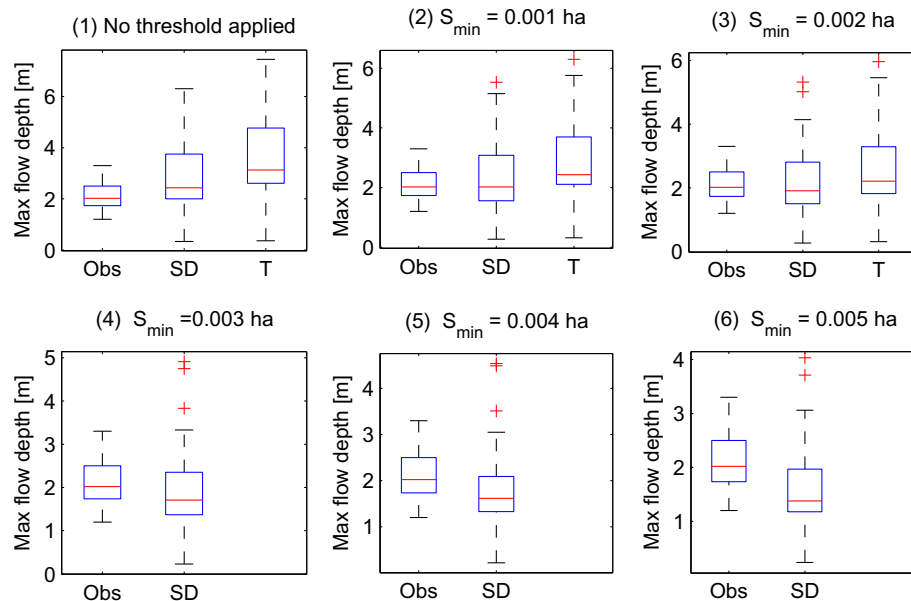


Fig. 12. Comparison of the maximum debris flow depth reproduction of the 1 October event for all six scenarios in terms of the box-and-whiskers-plot for the traditional and the proposed spatially-distributed methodology. The box width is equal to the interquartile range and the central value indicates the median value, data outside the whiskers are “out-of-range” values. These plots compare observed-simulated flow depth pairs measured at the same locations, and are obtained from data shown in Table 3.

Table 4

Unstable volume estimation for the Loco basin using: TRIGRS model, pre-event and post event DEM (Ventisette et al., 2012), and several empirical formula (Bianco and Franzi, 2000; Bottino et al., 1996; Kronfellner-Kraus, 1984; Marchi and Tecca, 1996; Tropeano and Turconi, 1999).

Applied methods	Volume [m ³]
TRIGRS model	11060
Ventisette et al. (2012)	13,507
Bianco and Franzi (2000)	3829
Bottino et al. (1996)	12,008
Kronfellner-Kraus (1984)	7184
Marchi and Tecca (1996)	9129
Tropeano and Turconi (1999)	83,262

4. Conclusions

Modelling debris flow triggering and propagation provides useful tools for susceptibility mapping, an important step for risk mitigation in landslide prone areas. Here a methodology for debris-flow modelling has been proposed, which couples a spatially distributed map of potential unstable areas and the subsequent propagation and deposition of the triggered masses. To this end, a simple and general empirical framework for combining triggering and propagation models has been devised in the paper; the framework is one step toward improving commonly-applied debris flow susceptibility methods, where the triggered mass is estimated by simply incrementing the flood hydrograph by a more or less empirical multiplier that accounts for the presence of the solid phase. The latter approach presents various drawbacks, mainly related to the fact that the destabilized sediment masses are prescribed as input at points chosen empirically and arbitrarily. In addition this lumped approach is strongly basin specific, i.e. depends on the draining basin on which the flood hydrograph is computed.

One crucial step of the proposed methodology is the definition of the landslide instability-to-debris flow triggering threshold, to identify those cells, among the potentially unstable ones resulting from the application of the hydrological-geotechnical models, that effectively contribute to debris flow. This threshold may be deter-

mined successfully by using data available from past events (inundated areas map and spatial distribution of maximum flow depths). To this aim receiver-operating characteristics (ROC) analysis and statistical tools that allow to compare the simulated maximum flow depths with those observed have been used. The calibrated instability-to-debris flow triggering threshold may be used to perform predictive susceptibility mapping in nearby areas that present similar soil hydraulic and geo-mechanical properties. The proposed approach has led to promising results, which may be improved by a multi-parametric optimization and model sensitivity analysis respect to uncertain soil parameter values.

Simulation of the Giampilieri event occurred on 1 October 2009, leads to a generally good agreement with observations. Nonetheless, the procedure still has some limitations, including a) the infinite slope stability analysis on which the TRIGRS model is based, which generally tends to overestimate unstable cells, since it neglects lateral strength, b) lack of accounting for erosion processes in high slope region, in the FLO-2D model, that brings to underestimate the volume of the propagation mass. Thus there are still margins of improvement, as suggested by the ROC indexes. The proposed spatially distributed hydrograph approach is found to produce robust and reliable results, especially when assessing susceptibility in the urban area. Moreover, the use of a spatially distributed model for the estimation of the triggered cells, being more consistent with the real process, may lead to better results in the upper parts of the basin where the triggering takes place.

Acknowledgments

This research was partially funded by the Italian Education, University and Research Ministry (MIUR), PON project No. 01_01503 Integrated Systems for Hydrogeological Risk Monitoring, Early Warning and Mitigation Along the Main Lifelines, CUP B31H11000370005, and through the Research projects of significant national interest – PRIN 2010–2011 – project name HYDRO-CAR (cod. 20104/2Y8M.003), and the PRIN 2012 project Project “Hydro-morphodynamics modelling of coastal processes for engineering purposes” (cod. 2012BY_TPR5). The research was also funded by the European Commission, project HYDRALAB PLUS

(proposal number 654110) and through the PO FESR SICILIA 2007–2013, Axes IV, Project MedNETNA. All consultants of the OPCM 10th October 2009 No.3815 are greatly acknowledged for the support demonstrated and for the useful information provided. We would like to thank the Public Civil Engineering Works Office of Messina and the Department of Civil Defence of Sicilian Region for providing important data. Finally, the authors thank Martin Mergili and other two anonymous reviewers for the useful suggestions and revisions that helped to improve significantly the manuscript.

References

- Anagnostopoulos, G.G., Fatchi, S., Burlando, P., 2015. An advanced process-based distributed model for the investigation of rainfall-induced landslides: the effect of process representation and boundary conditions. *Water Resour. Res.* 51 (9), 7501–7523.
- Baum, R.L., Godt, J.W., Savage, W.Z., 2010. Estimating the timing and location of shallow rainfall-induced landslides using a model for transient, unsaturated infiltration. *J. Geophys. Res.* 115, F03013.
- Baum, R.L., Savage, W.Z., Godt, J.W., 2002. TRIGRS – A FORTRAN Program for Transient Rainfall Infiltration and Grid-Based Regional Slope-Stability Analysis. U.S. Geological Survey Open-File Report 02-0424, Reston, Virginia.
- Baum, R.L., Savage, W.Z., Godt, J.W., 2008. TRIGRS – A FORTRAN program for transient rainfall infiltration and grid-based regional slope-stability analysis, version 2.0. U.S. Geological Survey Open-File Report 2008-1159, Reston, Virginia.
- Bellugi, D., Milledge, D.G., Dietrich, W.E., McKean, J.A., Perron, J.T., Sudderth, E.B., Kazian, B., 2015. A spectral clustering search algorithm for predicting shallow landslide size and location. *J. Geophys. Res.: Earth Surface* 120 (2), 300–324.
- Bianco, G., Franz, L., 2000. Estimation of debris flow volumes from storm events. In: *Proceedings of Debris Flow Mitigation: Mechanics, Prediction and Assessment*, Taipei, Taiwan, pp. 441–448.
- Blahut, J., Horton, P., Sterlacchini, S., Jaboyedoff, M., 2010. Debris flow hazard modelling on medium scale: Valtellina di tirano, Italy. *Natural Hazards Earth Syst. Sci.* 10 (11), 2379–2390.
- Bogaard, T.A., Greco, R., 2016. Landslide hydrology: from hydrology to pore pressure. *Wiley Interdiscip. Rev. Water* 3 (3), 439–459. <http://dx.doi.org/10.1002/wat2.1126>.
- Borga, M., Dalla Fontana, G., Cazorzi, F., 2002. Analysis of topographic and climatic control on rainfall-triggered shallow landsliding using a quasi-dynamic wetness index. *J. Hydrol.* 268 (1–4), 56–71.
- Bottino, G., Crivellari, R., Mandrone, G., 1996. Eventi pluviometrici critici e dissesti: individuazione delle soglie di innescio di colate detritiche nell'anfiteatro morenico di ivrea. In: *Proceedings of La prevenzione delle catastrofi idrogeologiche: il contributo alla ricerca scientifica*, Alba (Torino), pp. 201–210.
- Brönnimann, C., Stähli, M., Schneider, P., Seward, L., Springman, S.M., 2013. Bedrock exfiltration as a triggering mechanism for shallow landslides. *Water Resour. Res.* 49 (9), 5155–5167. <http://dx.doi.org/10.1002/wrcr.20386>.
- D'Odorico, P., Fagherazzi, S., Rigon, R., 2005. Potential for landsliding: dependence on hyetograph characteristics. *J. Geophys. Res. Earth Surface* 110 (F1).
- Fan, L., Lehmann, P., Or, D., 2016. Effects of soil spatial variability at the hillslope and catchment scales on characteristics of rainfall-induced landslides. *Water Resour. Res.* 52 (3), 1781–1799. <http://dx.doi.org/10.1002/2015WR017758>.
- Farahmand, A., AghaKouchak, A., 2013. A satellite-based global landslide model. *Nat. Hazards Earth Syst. Sci.* 13 (5).
- Foti, E., Faraci, C., Scandura, P., Cancelliere, A., La Rocca, C., Musumeci, R.E., Nicolosi, V.M., Peres, D., Stancanelli, L.M., 2013. Da giampilieri a saponara: analisi delle cause scatenanti e delle cause predisponenti. *Atti Dei Convegni Lincei-Accademia Nazionale Dei Lincei* 270, 45–64.
- Frattini, P., Crosta, G., Carrara, A., 2010. Techniques for evaluating the performance of landslide susceptibility models. *Eng. Geol.* 111 (1–4), 62–72.
- Highland, L.M., Bobrowsky, P., 2008. The landslide handbook - A guide to understanding landslides. Tech. Rep. 1325, U.S. Geological Survey, Reston, Virginia, 129 p.
- Horton, P., Jaboyedoff, M., Rudaz, B., Zimmermann, M., 2013. Flow-r, a model for susceptibility mapping of debris flows and other gravitational hazards at a regional scale. *Nat. Hazards Earth Syst. Sci.* 13 (4), 869–885.
- Hürlimann, M., Rickenmann, D., Medina, V., Bateman, A., 2008. Evaluation of approaches to calculate debris-flow parameters for hazard assessment. *Eng. Geol.* 102 (3), 152–163.
- Iverson, R.M., 2000. Landslide triggering by rain infiltration. *Water Resour. Res.* 36, 1897–1910.
- Jakob, M., 2005. Debris-Flow Hazard Analysis. In: *Debris-flow Hazards and Related Phenomena*. Springer, pp. 411–443.
- Kritikos, T., Davies, T., 2014. Assessment of rainfall-generated shallow landslide/debris-flow susceptibility and runoff using a gis-based approach: application to western southern alps of new zealand. *Landslides* 12 (6), 1051–1075. <http://dx.doi.org/10.1007/s10346-014-0533-6>.
- Kronfeller-Kraus, G., 1984. Extreme feststofffrachten und grabenbildungen von wildbächen [extreme sediment loads and erosion of torrents]. In: *Proceedings of International Symposium Interpraevent*, pp. 109–118.
- Lanni, C., McDonnell, J., Hopp, L., Rigon, R., 2013. Simulated effect of soil depth and bedrock topography on near-surface hydrologic response and slope stability. *Earth Surf. Proc. Land* 38 (2), 146–159. <http://dx.doi.org/10.1002/esp.3267>.
- Lanzoni, S., Gregoretti, C., Stancanelli, L.M., 2017. Coarse-grained debris flow dynamics on erodible beds. *J. Geophys. Res. Earth Surface* 122, 592–614. <http://dx.doi.org/10.1002/2016JF004046>.
- Lehmann, P., Or, D., 2012. Hydromechanical triggering of landslides: from progressive local failures to mass release. *Water Resour. Res.* 48 (3).
- Marchi, L., Arattano, M., Deganutti, A.M., 2002. Ten years of debris-flow monitoring in the moscardo torrent (Italian alps). *Geomorphology* 46 (1–2), 1–17. URL <http://www.sciencedirect.com/science/article/pii/S0169555X01001623>.
- Marchi, L., Tecca, P., 1996. Magnitudo delle colate detritiche nelle alpi orientali italiane. *Geingegneria Ambientale e Mineraria* 33 (2/3), 79–86.
- Mergili, M., Fellin, W., Moreiras, S.M., Stötter, J., 2012. Simulation of debris flows in the central andes based on open source gis: possibilities, limitations, and parameter sensitivity. *Nat. Hazards* 61 (3), 1051–1081.
- Milledge, D.G., Bellugi, D., McKean, J.A., Densmore, A.L., Dietrich, W.E., 2014. A multidimensional stability model for predicting shallow landslide size and shape across landscapes. *J. Geophys. Res. Earth Surface* 119 (11), 2481–2504.
- Montgomery, D.R., Dietrich, W.E., 1994. A physically based model for the topographic control on shallow landsliding. *Water Resour. Res.* 30, 1153–1171.
- Murphy, A., 1996. The finley affair: a signal event in the history of forecast verification. *Weather and Forecasting* 11 (1), 3–20.
- O'Brien, J., 1986. Physical Processes, Rheology and Modeling of Mudflows. Colorado State University. Doctor of Philosophy dissertation.
- O'Brien, J., 2006. Flo-2d user's manual. version 2006.01, flo-2d software. Inc., Nutrioso.
- O'Brien, J.S., Julien, P.Y., 1988. Laboratory analysis of mudflow properties. *J. Hydraul. Eng.* 114 (8), 877–887.
- Park, D., Nikhil, N., Lee, S., 2013. Landslide and debris flow susceptibility zonation using trigs for the 2011 seoul landslide event. *Nat. Hazards Earth Syst. Sci.* 13 (11), 2833–2849.
- Peres, D., Cancelliere, A., 2014. Derivation and evaluation of landslide-triggering thresholds by a Monte Carlo approach. *Hydrol. Earth Syst. Sci.* 18 (12), 4913–4931.
- Peres, D.J., Cancelliere, A., 2016. Estimating return period of landslide triggering by Monte Carlo simulation. *J. Hydrol.* 541 (Part A), 256–271. <http://dx.doi.org/10.1016/j.jhydrol.2016.03.036>.
- Peres, D.J., Cancelliere, A., 2014. Derivation and evaluation of landslide-triggering thresholds by a Monte Carlo approach. *Hydrol. Earth Syst. Sci.* 18 (12), 4913–4931.
- Rickenmann, D., Laigle, D., McArdell, B., Hübl, J., 2006. Comparison of 2d debris-flow simulation models with field events. *Comput. Geosci.* 10 (2), 241–264.
- Rickenmann, D., Zimmermann, M., 1993. The 1987 debris flows in Switzerland: documentation and analysis. *Geomorphology* 8 (2), 175–189.
- Rosso, R., Rulli, M.C., Vannucchi, G., 2006. A physically based model for the hydrologic control on shallow landsliding. *Water Resour. Res.* 42 (6), 1–16.
- Salciarini, D., Godt, J.W., Savage, W.Z., Baum, R.L., Conversini, P., 2008. Modeling landslide recurrence in Seattle, Washington, USA. *Eng. Geol.* 102 (3–4), 227–237.
- Schilirò, L., Esposito, C., Scarascia Mugnozza, G., 2015. Evaluation of shallow landslide-triggering scenarios through a physically based approach: an example of application in the southern Messina area (northeastern sicily, Italy). *Nat. Hazards Earth Syst. Sci.* 15 (9), 2091–2109.
- Sidele, R.C., Ochiai, H. (Eds.), 2006. Landslides: Processes, Prediction, and Land Use. American Geophysical Union Water Resources Monograph 18, AGU.
- Stancanelli, L., Foti, E., 2015. A comparative assessment of two different debris flow propagation approaches—blind simulations on a real debris flow event. *Nat. Hazards Earth Syst. Sci.* 15 (4), 735–746.
- Stancanelli, L., Lanzoni, S., Foti, E., 2014. Mutual interference of two debris flow deposits delivered in a downstream river reach. *J. Mt. Sci.* 11 (6), 1385–1395.
- Stancanelli, L., Lanzoni, S., Foti, E., 2015. Propagation and deposition of stony debris flows at channel confluences. *Water Resour. Res.* 51 (7), 5100–5116.
- Takahashi, T., 1981. Estimation of potential debris flows and their hazardous zones: soft countermeasures for a disaster. *Nat. Disaster Sci.* 3 (1), 57–89.
- Tarolli, P., Borga, M., Chang, K.-T., Chiang, S.-H., 2011. Modeling shallow landsliding susceptibility by incorporating heavy rainfall statistical properties. *Geomorphology* 133 (3–4), 199–211.
- Taylor, D., 1948. Fundamentals of Soil Mechanics. John Wiley, New York.
- Tropeano, D., Turconi, L., 1999. Valutazione del potenziale detritico in piccoli bacini delle Alpi Occidentali e Centrali. CNR-IRPI/GNDICI, Pubbl. n. 2058 Linea 1.
- Ventisette, C.D., Garfagnoli, F., Ciampalini, A., Battistini, A., Gigli, G., Moretti, S., Casagli, N., 2012. An integrated approach to the study of catastrophic debris-flows: geological hazard and human influence. *Nat. Hazards Earth Syst. Sci.* 12 (9), 2907–2922.